Topology and Routing Optimization Problem in Wireless Optical Networks

Itong Wijoko
itong.wijoko.077@lu.se

Department of Electrical and Information Technology
Lund University

Advisor: Prof. Michal Pióro

April 3, 2013

Printed in Sweden
E-huset, Lund, 2013

Abstract

Optical Fiber (OF) is a common solution to build optical links in Metropolitan Area Networks (MAN) backbones. Such fiber links can be leased from an optical transmission carrier by a MAN operator. Free Space Optics (FSO) can potentially decrease the MAN operating cost by substituting (partly or fully) the OF links by the FSO links. Although using only FSO links can be substantially cheaper, using FSO links has also a number of drawbacks since an FSO link requires two sites that are in the line of sight, is limited in distance, and affected by weather conditions. These factors make FSO links not as reliable as OF links, and thus, in general FSO networking can be more expensive than OF networking as the network topology of the former must be at least two-connected.

Therefore, identifying a subset of OF links that could be substituted by a set of FSO links in a cost efficient way, placement of the links, and identifying the demand routing, in order to minimize the total cost of the network is an optimization problem that is called Joint Topology and Routing Optimization Problem (JTROP). In the thesis an optimization approach for JTROP is developed, implemented and run on a set of network examples. The numerical results show that JTROP is capable of improving the pure FSO link solution when two-connectivity of a network is required.

Keywords: OF, FSO, LOS, topology, optimization, disjoint-path, two-connectivity.

Table of Contents

List of Figures

List of Tables

Chapter 1

Introduction

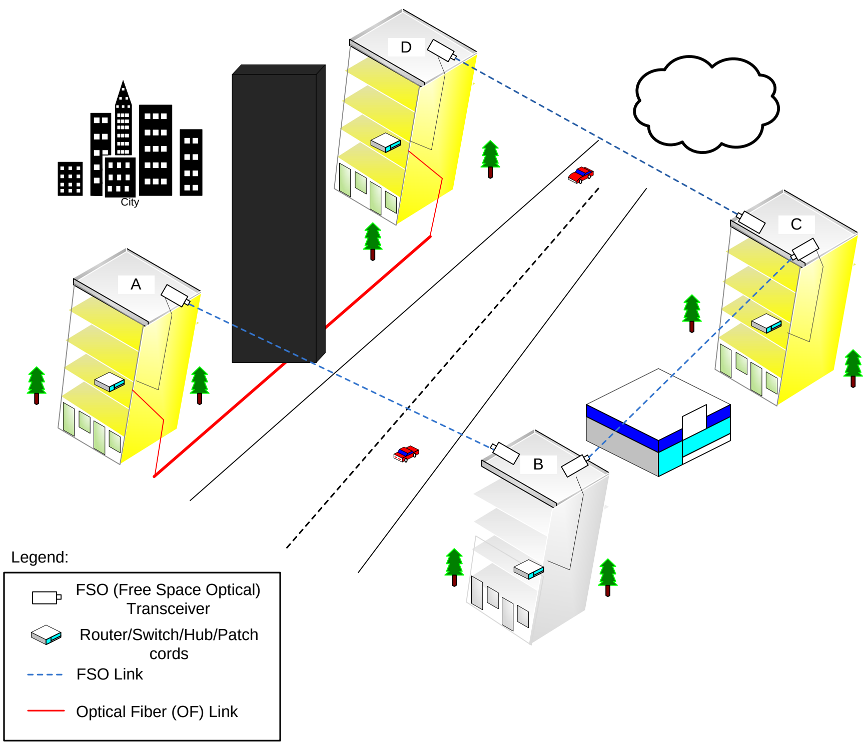

Figure 1.1: FSO MANs Communication Overview.

In this thesis we study design problems related to mesh optical backbones of Metropolitan Area Networks (MAN). Today, a common solution is to use the optical fiber paths to build optical links of the backbone. Such fiber links can be for an example leased from an optical transmission carrier by a MAN operator. Certainly, one of the main cost factors of this solution for a MAN operator is incurred by a (monthly, yearly) cost of leasing the optical links of a given capacity (bandwidth).

A recent optical transmission technology, known as Free Space Optics (FSO), can potentially decrease the MAN operating cost by substituting (partly or fully) optical fiber (OF) links by FSO links. In such a mixed solution, each FSO link is realized between the transceivers installed on the roofs of the two buildings corresponding to the end nodes of the link, and used instead (or in parallel) of the OF link between these two nodes. In general, the use of an FSO link instead of a OF link of the same capacity (expressed in Gb/s) can be substantially cheaper in terms of its monthly cost calculated as the cost of the link installation and maintenance divided by its lifetime expressed in the number of months.

Certainly, although using FSO links instead of OF links can be substantially cheaper from the link perspective, using FSO links have a number of drawbacks. For example, an FSO link can be installed only between the two sites that are in the line of sight (LOS) and are not too far from each other. Also, the FSO links are not that reliable as OF links are, which has an impact on the network topology such as two-connectivity. These factors make the FSO networking more expensive than the OF networking, because in general more links must be installed. But FSO is in general less expensive.

Thus, using FSO links in the MAN optical backbone introduces a trade-off between decreasing the overall link cost and increasing the topology cost. Therefore, identifying the subset of OF links that should be substituted by (in general a different, larger) set of FSO links in order to minimize the total cost of the network is an optimization problem, and this is the problem that we investigate in this thesis.

In the sequel the problem is called Joint Topology and Routing Optimization Problem (JTROP). In the thesis we formulate several variants of JTROP models, describe implementation of their resolution procedures (using an optimization package Gurobi), and apply them to a set of generated network instances studied within an extensive numerical study. From the numerical study we derive conclusions concerning the optimal solutions of JTROP for different sets of parameters including the cost factors relations, network size, allowable node degree, and so on.

The presented MSc project was motivated by the lack of similar studies in the accessible literature.

Connection between FSO and OF links is depicted in Figure 1.1.

1.1 Thesis Outline

The rest of thesis is organized as follows. In Chapter 1, problem description is briefly described and motivation is included.

In Chapter 2, we discuss the importance of design issues that potentially degrade FSO performance, such as the atmospheric channel loss and its turbulence a major contributor and other factors. The impact of the atmospheric conditions to the visibility for different wavelength is shown together with several atmospheric condition.

In Chapter 3, JTROP models are introduced. Notation and model formulations are presented. Starting from Basic formulation of JTROP, followed by Full JTROP for one-connected case, and continued with two-connected cases of JTROP for Basic and Full formulations.

In Chapter 4, several cases are investigated using two sets of randomly generated networks. Models performance is compared for several settings of the cost factors and allowable degree of the FSO nodes. Discussion is added for each implementation.

Finally, in Chapter 5, general conclusions are drawn and potential future work is highlighted.

Chapter 2

Free Space Optical Networks

2.1 Background

Development and implementation of FSO networks initially started for military purposes [4]. It is getting popular as a commercial application and is becoming one of the potential candidates for broadband wireless communications [3]. Ghasemlooy et.al., [4] and Willebrand et.al., [7] highlighted the benefits of FSO such as: free spectrum licenses, large bandwidth, long distance operations and easy installation and deployment.

These reasons make FSO suitable for implementation in local area networks (LAN), wide area networks (WAN) and also metropolitan area networks (MAN) [4]. In this thesis we focus our work on the MAN application.

As shown in Figure 2.1, the bandwidth of FSO ranges from 10^{12} to 10^{16} Hz, therefore it is clearly seen FSO has an enormous potential for operating bandwidth. It is also pointed out that OF frequency operating is inside the FSO frequency band. The free spectrum is due to the fact that The Federal Communications Commission (FCC) does not regulate frequency above 300 GHz [7].

In commercial applications, FSO systems operate using wavelength range around 785 nm and 1550 nm that is inside transmission windows. The reason is to reduce the free-space absorption [7]. However, OF is also using the same operating wavelength which makes them similar in terms of electrical/optical process conversion, enabling the transceiver components to be shared [7]. This direct compatibility is also one of our motivations.

The most significant difference between FSO and OF transmission is the operating media. OF uses guided channels that have predictable rate of cable attenuation such as $0.2 - 0.5$ dB/km for single-mode and $2 - 3$ dB/km for multi-mode [7][5].

On the other hand, FSO is transmitted at free space that experience atmospheric attenuation. The attenuation itself can vary from 0.2 dB/km in clear weather to 350 dB/km in dense fog, as shown in Figure 2.2; the high attenuation during very dense fog potentially reduce the up time and may even shutdown FSO links. This uncertainty is a main concern in acceptance of FSO [3] for resilient applications. However, the improvement of FSO unreliability is another motivation for this thesis.

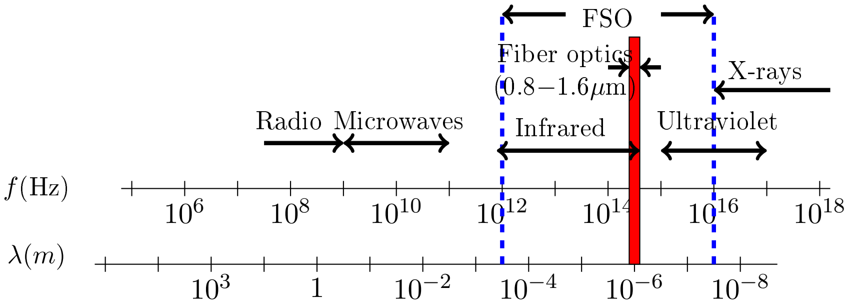

Figure 2.1: Spectrum of electromagnetic radiation [8].

2.2 Design Issues

This section briefly discusses factors that affect performance of FSO.

2.2.1 Freespace Channel Modeling

As described previously, FSO is heavily influenced by weather conditions as a consequence of operating in free-space. The particles in atmosphere are mainly nitrogen, oxygen and water vapor [4] which can scatter or absorb the propagated infrared photons [7].

2.2.1.1 Atmospheric Channel Attenuation

The atmospheric channel as a result of absorption and scattering processes attenuates the electromagnetic field traversing onto it. The concentration of particles in the atmosphere, depend on the current local weather conditions, which vary the attenuation of the transmission signal spatially and temporally [4]. Furthermore, the attenuation of FSO from transmitter to receiver is described by Beer-Lambert's law given as Equation(2.1) [4][7].

$$\tau(\lambda, R) = \frac{P_R}{P_T} = exp(-\alpha(\lambda)R) \tag{2.1}$$

where P_R is detected power intensity (in watt) at location R and P_T is initial transmitted power intensity (in watt). The ratio of them is also called transmittance [3]. Parameter $\alpha(\lambda)$, represents the total attenuation coefficient at certain wavelength. The received power is exponentially decreased with $\alpha(\lambda)$ and distance.

In addition, the total attenuation/extinction coefficient, $\alpha(\lambda)$ in m^{-1}, is the sum of the absorption and the scattering coefficients from particles constituents of the atmosphere [4]. The absorption is an interaction between the propagating photons and molecules along its path which is wavelength dependent. In order to reduce the effect of absorption, therefore as per suggested by Ghasemlooy et.al., [4], wavelength used is located within atmospheric transmission windows such as 785 nm and 1550 nm.

Scattering results in angular redistribution of the optical field with and without wavelength modification [4]. It depends on the radius, r, of the particles

Type	Radius(μm)	Size Parameterx_0	Scattering Process
Air Molecules	0.0001	0.00074	Rayleigh
Haze particle	0.01−1	0.074−7.4	Rayleigh − Mie
Fog droplet	1−20	7.4−147.8	Mie−Geometrical
Rain	100−10000	740−74000	Geometrical
Snow	1000−5000	7400−37000	Geometrical
Hail	5000−50000	37000−370000	Geometrical

Table 2.1: Typical atmospheric scattering particles with their radii and scattering process at λ= 850 nm [4].

encountered during propagation. One way of describing this is to consider the size parameter $x_0 = 2\pi r/\lambda$ [4]. If $x_0 \ll 1$ the scattering is classified as Rayleigh scattering, if $x_0 \approx 1$ it is Mie scattering and for $x_0 \gg 1$ the scattering process can then be explained using the diffraction theory (geometric optics), in detail can be found in [4][7]

As shown in Table 2.1 and Figure 2.2, it is obvious that fog is a major photon scatterer and it contributes as the major power attenuation [4].

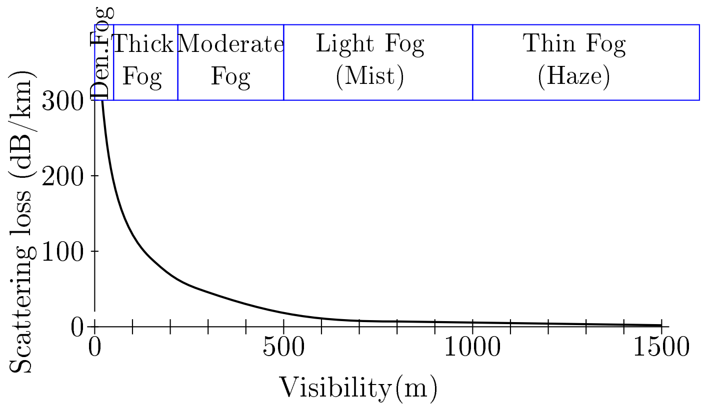

Figure 2.2: Atmospheric attenuation as function of visibility λ=785 nm [6].

As indicated in Figure 2.2 the visibility in dense fog for operating wavelength at 785 nm is very short it is around 50 meter and the attenuation is around 300 dB/km [6] where in practical application it can shut-down the FSO links.

Scattering caused by fog is categorized in Mie scattering. It is described based on empirical formula expressed in terms of the visibility range V in km as shown in Equation(2.2) [4].

$$\beta_a(\lambda) = \frac{3.91}{V}\left(\frac{\lambda}{550}\right)^{-\delta} \tag{2.2}$$

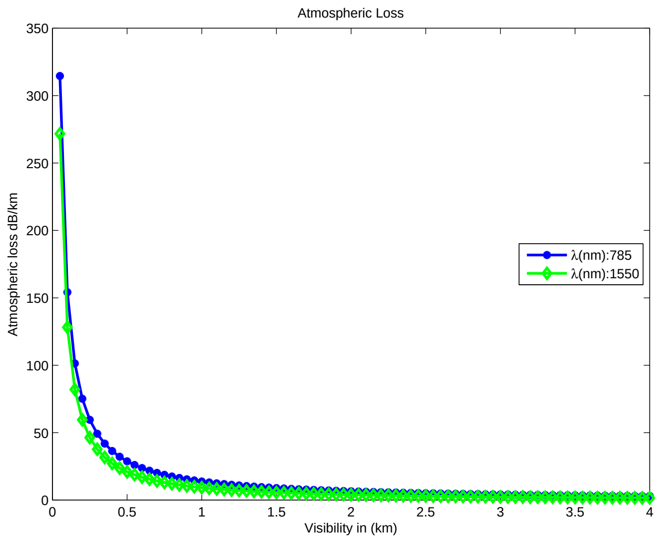

Figure 2.3: Comparasion atmospheric attenuation as function of visibility for λ=785 and 1550 nm [6].

where λ is wavelength in nm, β_a is atmospheric attenuation and δ is size of scattering particles defined by using Kim and Kruse model see [4][6].

As shown in Figure 2.3 that system uses wavelength 1550 nm is slightly less attenuated than the system with a lower wavelength at 785 nm. The scatter model used in Figure 2.3 is the Kruse model [4][6].

Attenuation caused by other scattering objects such as rain and snow are low compared to fog. Heavy rain attenuation is around 7 dB/km while attenuation from snow is around 34 dB/km [5].

For most commercial FSO deployments, operation in heavy fog environments requires keeping the distance between FSO transceiver to short distance in order to maintain the high levels of availability. The link power margin of most vendors equipment allow for availability that exceed 99.99% if distances are kept below 200 m [7].

2.2.1.2 Atmospheric Turbulence

Another parameter that effects the performance of FSO is refractive index structure, denoted as C_n^2, indicate the strength of the atmospheric turbulence [3]. It is a function of the altitude and wind speed effects [4].

Ghasemlooy et.al., [4] discusses atmospheric turbulence factors such as weather phenomena and scintillation by pressure, humidity, and temperature in detail. The severe weather condition will significantly affect performance of a free space link.

The channel models commonly used for atmospheric are log−normal, gamma−gamma [4][3]. Weak to moderate turbulence condition can be described in log−normal model, and gamma−gamma is for strong atmospheric turbulence [4]. In this thesis, log−normal is considered. The marginal distribution of light intensity fading induced by atmospheric turbulence can be statistically modeled as Equation(2.3) [3]:

$$f_I(I) = \frac{1}{2\sigma_x I\sqrt{2\pi}} exp\left\{-\frac{(ln(I) - ln(I_o))^2}{8\sigma_x^2}\right\} \tag{2.3}$$

where I_0 is the average received power intensity and σ_x^2 is the variance of the log amplitude fluctuation. The variance has the form Equation(2.4) [3]

$$\sigma_x^2 = 0.30545\left(\frac{2\pi}{\lambda}\right)^{7/6} C_n^2(\eta) z^{11/6} \tag{2.4}$$

where, λ, is wavelength in meter, $C_n^2(\eta)$, in is the index of refraction structure parameter in $m^{-2/3}$, with constant altitude η in meter, and z is the transmission distance in meter. For atmospheric channels near the ground, e.g., $\eta < 18.5$ m, C_n^2 ranges from $10^{-13}m^{-2/3}$ to $10^{-17}m^{-2/3}$ for strong to weak atmospheric turbulence, with a typical value $10^{-15}m^{-2/3}$. Under log-normal fading, the reliability of an FSO link can be computed as Equation(2.5) [3]:

$$\Gamma_{ij} = Pr\{I \geq I_{th}\} = \frac{1}{2} - \frac{1}{2} erf\left(\frac{(ln(I) - ln(I_o))^2}{2\sigma_x\sqrt{2}}\right) \tag{2.5}$$

where I_{th} is a threshold of received signal intensity. For fixed ratio of I_{th}/I_0, Γ_{ij} is determined by the standard deviation σ_x, which is strongly influenced by the weather condition (i.e., a decreasing function of $C_n^2(\eta)$. With a suitable threshold, I_{th}, Γ_{th}, the potential link visibility of an FSO link can be obtained.

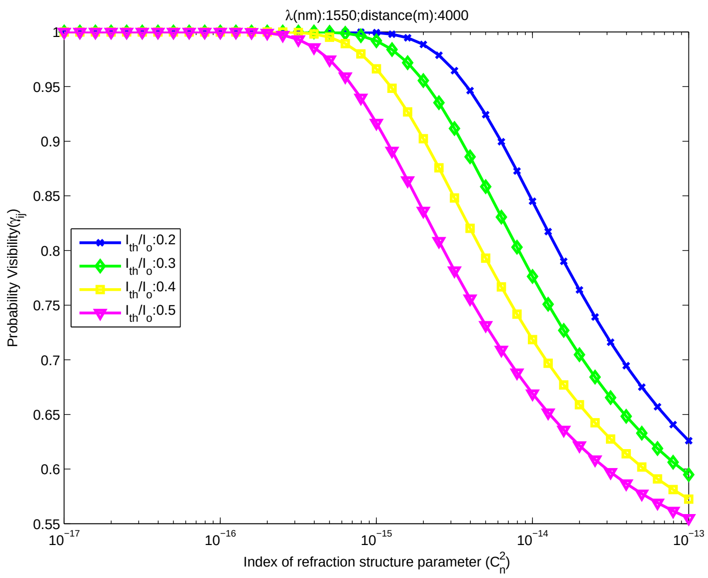

Figure 2.4: Link visibility (γ_{ij}) vs refraction coefficient (C_n^2) for different transmittance [3].

Figure 2.4 shows that the probability visibility of FSO link varies with atmospheric refraction turbulence at distance 4 km away from the transmitter using wavelength 1550 nm. It is clearly shown that the visibility link is varied and changed at different weather condition. A severe weather condition decreases the visibility of the links lower than 65% whereas at relatively clear weather (C_n^2=10^{-16}), the visibility link can reach up to around 5-nines (99.999%). The transmittance also defines the visibility. It makes sense that system with less attenuated intensity at receiver side (lower transmittance) has better visibility link compared to that system with higher attenuated intensity.

Furthermore, in Figure 2.5, at the same weather condition, visibility link of wavelength 1550 nm is greater than for a shorter wavelength. At C_n^2=10^{-16}, probability visibility of link for wavelength 1550 nm can reach above 90% whereas for wavelength 550 nm only about 80% for the same distance application. Equation(2.6) is used to define the potential of FSO link at certain level threshold.

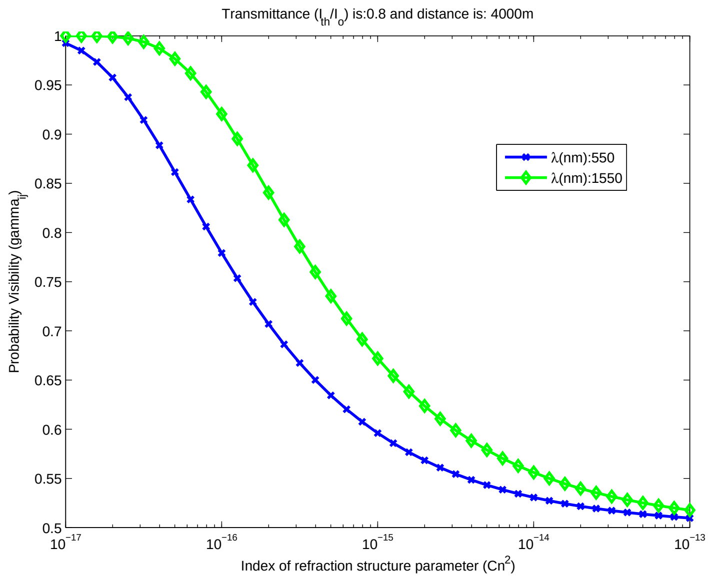

Figure 2.5: Link visibility (γ_{ij}) vs refraction coefficient (C_n^2), for different wavelength [3].

$$\omega(n) = \begin{cases} \Gamma_{ij} & \text{if } \Gamma_{ij} \geq \Gamma_{th} \\ 0 & \text{otherwise} \end{cases} \tag{2.6}$$

In this thesis, probability visibility of FSO link, Γ_{th} is set fixed at 90%.

2.2.2 Others Factors

Others attenuation factors (such as beam divergence due to beam diffraction, pointing loss is due to imperfect alignment of transmitter and receiver that can be caused by building sway, geometrical loss and also optical loss) are discussed in detail [4][7]. All these losses should be taken into account at link budget calculation in order to achieve the receiver sensitivity requirement.

2.2.3 Health and Safety

Transmitting with high power can certainly alleviate atmospheric losses influences, however, laser sources beyond certain power threshold can be dangerous to human body including eyes [3]. There are laser safety standards like ANSI Z136.1 and IEC 60825-1 [7]. According to IEC 60825-1(Amendment 2) the allowable transmitting power for 850 nm wavelength is 0.78 mW while for 1550 nm it is up to 10 mW, this because for wavelength 1550 nm the aqueous fluid of the eye absorbs much more of the energy of the beam, preventing it from traveling to the retina and inflicting damage. However, the cost production of 1550 nm is higher than for a shorter wavelength [7].

Chapter 3

Optimization Formulation Problems

3.1 JTROP – the one-connected case

In this section we will discuss the case of the joint topology and routing optimization problem (JTROP) that assumes no link/node failures. Therefore, the task is to install the links in the most cost effective way that assures one-connectivity between the end nodes of the connection demands.

3.1.1 Notation

The notation is as follows. The network of links is represented by an undirected graph G composed of the set of vertices (nodes) V and set of edges (links) E. A link $e \in E$ represents an undirected pair of two distinct vertices $\{v, w\}$ from V. The set of all edges in E incident with vertex $v \in V$ is denoted by $\delta(v)$. For a subset $A \subsetneq V$, $\delta(A)$ denotes the set of those edges that have exactly one vertex in A. Also, $E[A]$ will denote the subset of all edges in e with both ends in set A. If A, B are arbitrary sets of vertices $A, B \subseteq V(G)$ then $E(A, B)$ will denote the set of all edges between the two disjoint sets $A \setminus B$ and $B \setminus A$.

Connection demands are directed. A demand $d \in D$ (where $D \subseteq V^2 \setminus \{(v, v) : v \in V\}$ is the set of demands) is represented by a directed pair (s_d, t_d) of nodes.

In the node-link formulations of optimization tasks, it is required that the link flows are directed. Therefore, each link $e \in E, e = \{v, w\}$ is associated with two directed arcs $e' = (v, w)$ and $e'' = (w, v)$ with the arc flows (related to individual demands $d \in D$) denoted by $x_{e'd}$ and $x_{e''d}$. Consequently, $A = \{e', e'' : \ e \in E\}$ will denote the set all the so defined directed arcs of graph G with directed flows $x_{ad}, a \in A, d \in D$. For a node $v \in V$, $\delta^+(v)$ will denote the set of all directed arcs $a \in A$ outgoing from node v, and $\delta^-(v)$ – the set of all directed arcs $a \in A$ incoming to node v.

3.1.2 Basic formulation

The basic JTROP formulation is as follows:

$$\begin{aligned}
\min \quad & C = \textstyle\sum_{e \in E} \kappa_e u_e && && (3.1a)\\
& \sum_{a \in \delta^+(v)} x_{ad} - \sum_{a \in \delta^-(v)} x_{ad} = 0, && v \in V,\ d \in D && (3.1b)\\
& \sum_{a \in \delta^+(s_d)} x_{ad} - \sum_{a \in \delta^-(s_d)} x_{ad} = 1, && d \in D && (3.1c)\\
& x_{e'd} \le u_e,\ x_{e''d} \le u_e && e \in E && (3.1d)\\
& x_{ad} \ge 0, && a \in A && (3.1e)\\
& u_e \in \{0,1\}, && e \in E && (3.1f)
\end{aligned}$$

The vector of binary variables $u = (u_e :\ e \in E)$ indicates whether a link $e \in E$ is installed ($u_e = 1$) or not ($u_e = 0$). Hence, the objective function given by (3.1a) expresses the total cost of the installed links (where $\kappa_e,\ e \in E$ are the link installation costs). Equations(3.1b)-(3.1c) make sure that each demand $d \in D$ will be connected. Moreover, since for any fixed vector u, the polytope defined by (3.1b)-(3.1e) is totally unimodular, any flow solution $x = (x_{ad} :\ a \in A,\ d \in D)$ will be binary and hence will define a single path $p_d(x) = \{a \in A :\ x_{ad} = 1\}$ from s_d to t_d.

The so defined paths $p_d(x),\ d \in D$ may contain loops (even isolated). The loops can be easily eliminated by postprocessing the solution of(3.1). This is done by solving the following flow allocation problem for the given (optimal) u^*:

$$\begin{aligned}
\min \quad & C = \textstyle\sum_{a \in A} \sum_{d \in D} x_{ad} && && (3.2a)\\
& \sum_{a \in \delta^+(v)} x_{ad} - \sum_{a \in \delta^-(v)} x_{ad} = 0, && v \in V,\ d \in D && (3.2b)\\
& \sum_{a \in \delta^+(s_d)} x_{ad} - \sum_{a \in \delta^-(s_d)} x_{ad} = 1, && d \in D && (3.2c)\\
& x_{e'd} \le u^*_e,\ x_{e''d} \le u^*_e && e \in E && (3.2d)\\
& x_{ad} \ge 0, && a \in A && (3.2e)
\end{aligned}$$

The so obtained optimal paths $p_d(x^*),\ d \in D$ will be elementary.

3.1.3 Degree limit

In practice, the number of optical interfaces installed in the network nodes is limited. Let $b(v)$ ($v \in V$) denote the upper limit of the number of optical interface for node v. Then, this limiting requirement is taken into account by adding constraint

$$\sum_{e \in \delta(v)} u_e \le b(v), \quad v \in V \tag{3.3}$$

3.1.4 Node cost

Next, we introduce the cost of using the nodes by assuming the node costs χ_v, $v \in V$ (containing the rental cost of roofs of the buildings), adjusting the cost function

$$C = \sum_{e \in E} \kappa_e u_e + \sum_{v \in V} \chi_v U_v \tag{3.4}$$

(where U_v is the binary variable indication whether node $v \in V$ is installed) and by adding constraints

$$u_e \leq U_v, \quad v \in V,\ e \in \delta(v). \tag{3.5}$$

3.1.5 Fixed OF links

Now we modify JTROP by adding a possibility of using fixed IP links realized on optical fibers (OF). This is done by splitting the set of link E into two sets F (FSO links) and R (OF links). Clearly, $E = F \cup R$. With this extension, all the formulations given above remain unchanged except for the following. Constraint (3.5) becomes:

$$u_e \leq U_v^F, \quad v \in V,\ e \in \delta(v) \cap F \tag{3.6a}$$

$$u_e \leq U_v^r, \quad v \in V,\ e \in \delta(v), \tag{3.6b}$$

where $U_v^F, U_v^r, v \in V$ are binary variables indicating whether a node is incident to at least one FSO link ($U_v^F = 1$) and to at least one link (FSO or OF) ($U_v^r = 1$). Then, the objective (3.4) is modified accordingly:

$$C = \sum_{e \in E} \kappa_e u_e + \sum_{v \in V} (\chi_v^F U_v^F + \chi_v^r U_v^r). \tag{3.7}$$

Cost coefficient χ_v^F is interpreted as the cost of renting a space on the roof of the building related to node $v \in V$, and χ_v^r – as the cost of installing a router in that building.

Finally, we modify constraint (3.3)

$$\sum_{e \in \delta(v) \cap F} u_e \leq b(v), \quad v \in V. \tag{3.8}$$

3.1.6 Full JTROP formulation

The following problem summarizes all the above formulations and gives a general JTROP formulation assuring the cheapest, one-connected network configuration:

$$
\begin{aligned}
\min \quad & C = \textstyle\sum_{e \in E} \kappa_e u_e + \sum_{v \in V} (\chi_v^F U_v^F + \chi_v^r U_v^r) && && (3.9a) \\
& \sum_{a \in \delta^+(v)} x_{ad} - \sum_{a \in \delta^-(v)} x_{ad} = 0, && v \in V,\ d \in D && (3.9b) \\
& \sum_{a \in \delta^+(s_d)} x_{ad} - \sum_{a \in \delta^-(s_d)} x_{ad} = 1, && d \in D && (3.9c) \\
& x_{e'd} \le u_e,\ x_{e''d} \le u_e && e \in E && (3.9d) \\
& \sum_{e \in \delta(v) \cap F} u_e \le b(v) && v \in V && (3.9e) \\
& u_e \le U_v^F, && v \in V,\ e \in \delta(v) \cap F && (3.9f) \\
& u_e \le U_v^r, && v \in V,\ e \in \delta(v) && (3.9g) \\
& x_{ad} \ge 0, && a \in A && (3.9h) \\
& u_e \in \{0, 1\}, && e \in E && (3.9i) \\
& U_v^F \ge 0, U_v^r \ge 0, && v \in V && (3.9j)
\end{aligned}
$$

We note that eliminating of loops can be done in the same way as described above, and that variables $U^F = (U_v^F : v \in V)$ and $U^r = (U_v^r : v \in V)$ can be assumed continuous as in the optimal solution they will assume binary values automatically.

3.2 JTROP – the two-connected case

In this section we will discuss the case of the joint topology and routing optimization problem (JTROP) that assumes failure of the FSO links. Therefore, the task is to install the links in the most cost effective way that assures two-connectivity between the end nodes of the connection demands.

3.2.1 Basic two-connected formulation

The basic formulation giving below assures two-connectivity of demands. When only FSO links are used ($R = \emptyset$) which are subject to failures, two-connectivity means that each demand $d \in D$ is provided with two link-disjoint paths. The resulting formulation is as follows:

$$\min \quad C = \textstyle\sum_{e \in E} \kappa_e u_e \tag{3.10a}$$

$$\sum_{a \in \delta^+(v)} x_{ad} - \sum_{a \in \delta^-(v)} x_{ad} = 0, \qquad v \in V,\ d \in D \tag{3.10b}$$

$$\sum_{a \in \delta^+(s_d)} x_{ad} - \sum_{a \in \delta^-(s_d)} x_{ad} = 2, \qquad d \in D \tag{3.10c}$$

$$x_{e'd} \leq u_e,\ x_{e''d} \leq u_e \qquad e \in E \tag{3.10d}$$

$$x_{ad} \geq 0, \qquad a \in A \tag{3.10e}$$

$$u_e \in \{0, 1\}, \qquad e \in E \tag{3.10f}$$

Now, Equations (3.10b)-(3.10c), together with (3.11d), make sure that each demand $d \in D$ will be two-connected. Since for any fixed vector u, the polytope defined by (3.1b)-(3.1e) is totally unimodular, any flow solution $x = (x_{ad} :\ a \in A,\ d \in D)$ will be binary and hence will define a pair of link-disjoint paths $p_d(x) \cup q_d(x) = \{a \in A :\ x_{ad} = 1\}$ from s_d to t_d.

The so defined pairs of paths $(p_d(x), q_d(x))$, $d \in D$ may contain loops (even isolated). The loops can be easily eliminated by postprocessing of the solution of the considered problem (3.1). This is done by solving the following flow allocation problem for the given (optimal) u^*:

$$\min \quad C = \textstyle\sum_{a \in A} \sum_{d \in D} x_{ad} \tag{3.11a}$$

$$\sum_{a \in \delta^+(v)} x_{ad} - \sum_{a \in \delta^-(v)} x_{ad} = 0, \qquad v \in V,\ d \in D \tag{3.11b}$$

$$\sum_{a \in \delta^+(s_d)} x_{ad} - \sum_{a \in \delta^-(s_d)} x_{ad} = 2, \qquad d \in D \tag{3.11c}$$

$$x_{e'd} \leq u^*_e,\ x_{e''d} \leq u^*_e \qquad e \in E \tag{3.11d}$$

$$x_{ad} \geq 0, \qquad a \in A \tag{3.11e}$$

The so obtained optimal paths $p_d(x^*), q_d(x^*)$ will be elementary and disjoint for each given $d \in D$.

3.2.2 Full two-connected JTROP formulation

A full two-connected JTROP formulation taking into account node degree limits, node costs, and fixed fiber links is as follows:

$$\min \quad C = \textstyle\sum_{e\in E} \kappa_e u_e + \sum_{v\in V} (\chi_v^F U_v^F + \chi_v^r U_v^r) \tag{3.12a}$$

$$\sum_{a\in\delta^+(v)} x_{ad} - \sum_{a\in\delta^-(v)} x_{ad} = 0, \qquad v \in V,\ d \in D \tag{3.12b}$$

$$\sum_{a\in\delta^+(s_d)} x_{ad} - \sum_{a\in\delta^-(s_d)} x_{ad} = 2, \qquad d \in D \tag{3.12c}$$

$$x_{e'd} \le u_e,\ x_{e''d} \le u_e \qquad e \in E_w \tag{3.12d}$$

$$x_{e'd} \le 2u_e,\ x_{e''d} \le 2u_e \qquad e \in E_f \tag{3.12e}$$

$$\sum_{e\in\delta(v)\cap F} u_e \le b(v) \qquad v \in V \tag{3.12f}$$

$$u_e \le U_v^F, \qquad v \in V,\ e \in \delta(v) \cap F \tag{3.12g}$$

$$u_e \le U_v^r, \qquad v \in V,\ e \in \delta(v) \tag{3.12h}$$

$$x_{ad} \ge 0, \qquad a \in A \tag{3.12i}$$

$$u_e \in \{0,1\}, \qquad e \in E \tag{3.12j}$$

$$U_v^F \ge 0, U_v^r \ge 0 \qquad v \in V \tag{3.12k}$$

Note that the pair paths $(p_d(x^*), q_d(x^*))$ for any given $d \in D$ do not have to be link-disjoint with respect to fixed fiber links $e \in R$ since the fixed OF links are assumed to be 100% reliable. We note that loops eliminating can be done in the same way as described above.

Chapter 4

Numerical Study and Results

Having described the models in the previous chapter, in this chapter the optimization results for different sets of cases will be evaluated, followed by a discussion of the results.

4.1 Optimization Schema Overview

Network topologies are generated using a random data generator in the x-y plane. The codes for optimization models are developed in a Python environment. The optimization solver is a commercial package, GUROBI, a Mixed Integer Linear Programming problems (MILP) whose MILP solver is based on a branch-and bound algorithm involves LP. (For the details of GUROBI see [9]).

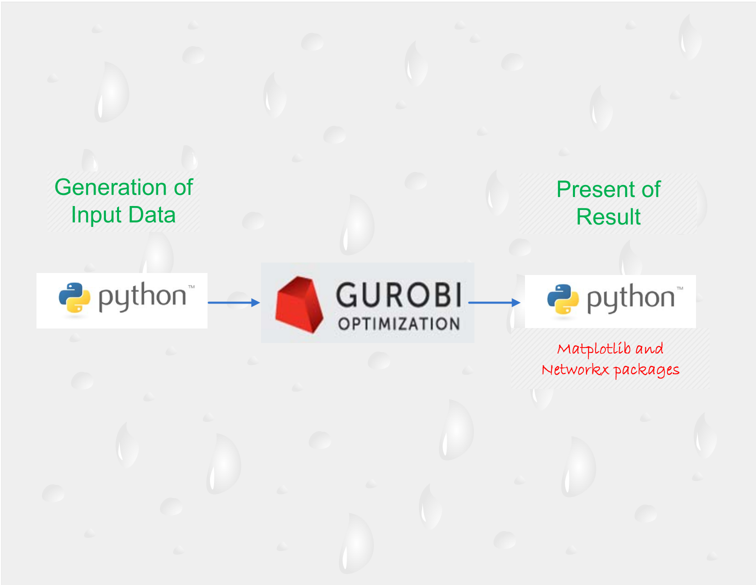

Figure 4.1: JTROP Optimization diagram.

The results of the solver are collected by the Python program and presented as figures by Matplotlib and Networkx packages. The processing overview is depicted in Figure 4.1. During each phase of the processes the output is saved into files.

The tests were conducted on AMD $Athlon^{TM}$ 64 X2 Dual Core Processor 5200+ with 1.8Gb of RAM running on 32 bits operating system.

There are two sets of randomized network data investigated in an area around 5 km^2 with different network topologies. Each set consists of 5 - 15 nodes. In the data, atmospheric condition is considered for the FSO links visibility besides obstacle objects. Wavelength, λ, used is 1550 nm and atmospheric condition is considered moderate with refraction coefficient,$C_n^2 = 1.5.10^{-14}$ for first set and with coefficient $C_n^2 = 1.10^{-14}$ for second one. Transmittance ratio, I_{th}/I_o, is 0.4, and visibility factor, Γ_{ij}, is defined as 0.9. Figure 4.2 shows that the visibility range for the first set is around 1300 meters while it is around 1700 meters for the second set. Therefore, the distance more than the visibility range is considered unavailable for the FSO links.

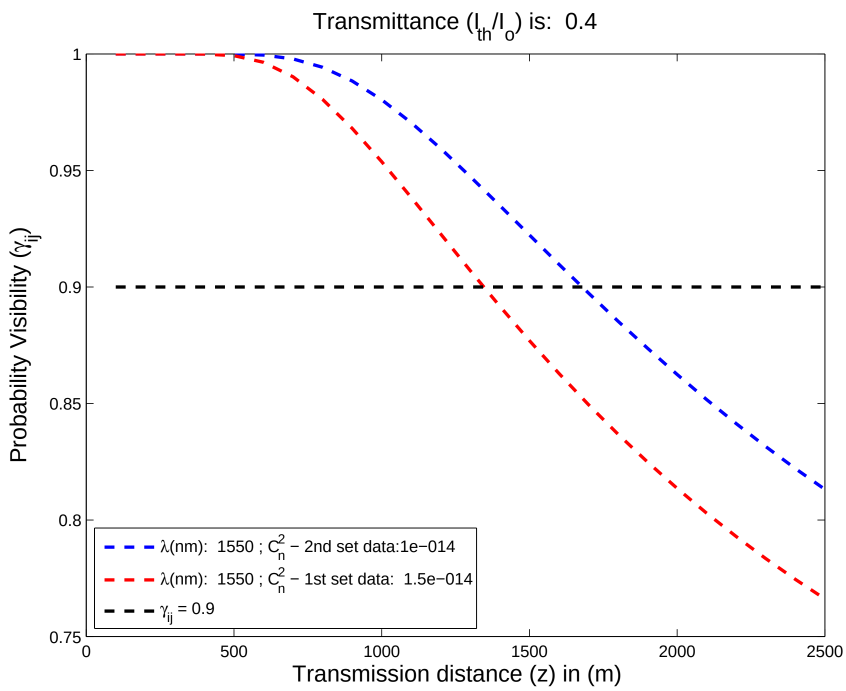

Figure 4.2: Transmission distance at $\lambda = 1550$ nm for $C_n^2 = 10^{-14}$ and $C_n^2 = 1.5.10^{-14}$.

4.1.1 Network Instances

Tables 4.1 and 4.2 list the network size of the random network data. Generally the number of potential FSO links and OF links increases with the increment of network size. Obstacles between the FSO transceivers obviously decrease the number of the FSO links.

Atmospheric conditions for first set of data is rougher than the second set, therefore first set of data in generally have less potential FSO links than second set for the same size of networks.

To ensure the connectivity a path is established between the nodes of each demand pairs. Since there are no customer premises at transit nodes there is no demand associated with transit nodes. Thus, number of demands for the network topology $\binom{n-t}{2}$, where n is the number of nodes and t is the number of transit nodes.

Nodes(n)	FSO links with obstacles	FSO links w/o obstacles	OF links	Demands
5	8	10	10	6
6	13	14	15	10
7	12	14	21	15
8	15	17	28	21
9	19	19	36	28
10	14	15	45	28
11	22	23	55	36
12	27	28	66	45
13	21	22	78	55
14	26	28	91	66
15	21	23	105	66

Table 4.1: Set1 Information, transmission distance at $\lambda = 1550$ nm for $C_n^2 = 1.5.10^{-14}$.

Nodes(n)	FSO links with obstacles	FSO links w/o obstacles	OF links	Demands
5	7	8	10	6
6	9	11	15	10
7	10	12	21	15
8	17	18	28	21
9	21	24	36	28
10	28	31	45	28
11	30	35	55	36
12	36	38	66	45
13	48	51	78	55
14	52	55	91	66
15	54	59	105	66

Table 4.2: Set2 Information, transmission distance at $\lambda = 1550$ nm for $C_n^2 = 1.10^{-14}$.

4.2 Case Studies and Discussions

In order to evaluate the performance of models, we investigated some cases by changing the cost parameters of the models. Computational time and objective function are recorded for discussion.

4.2.1 Case-1: Cost χ_v^F= 1 , Cost χ_v^r=1, and $b(v)$=4

In this case, the leased building (in actual is in USD), χ_v^F, and router equipment, χ_v^r, costs have the same price as FSO transceivers and the FSO transceiver link is limited to degree 4. Figure 4.3 shows the network topology with two transit nodes. The left hand side is the topology without obstacles while the right hand side considers it with obstacles is present.

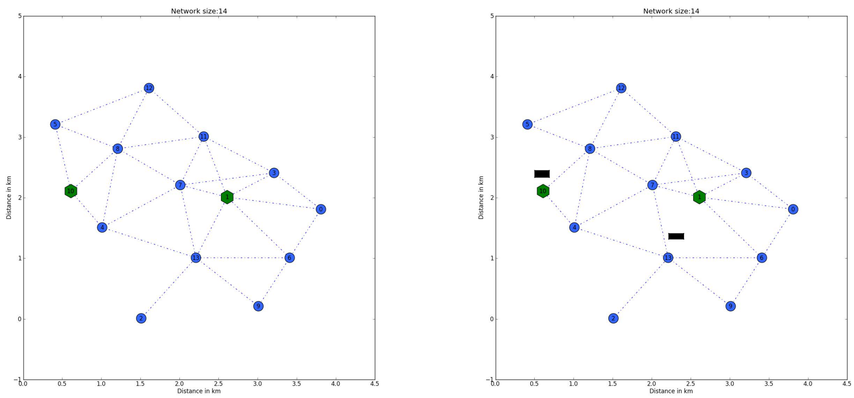

(a) Network instance with no obstacles, number of nodes = 14.

(b) Network instances with obstacles, number of nodes = 14.

Figure 4.3: Network overview, circle is node, diamond is transit node, dotted line is FSO link and rectangular is obstacle object.

The performance of the models is compared in Figure 4.4. In the upper part it shows the objective cost against the number of nodes of one-connectivity as well as two-connectivity models. It is observed that the objective is grouped into two parts, one for full connected at higher curves another for basic connected at lower curves. Accumulated cost is increased as number of connected nodes are increased . It is reasonable that objective cost for full connected models are more expensive than basic connected since the price of leased building and routers equipment are considered for full connected while on basic connected is only considering the link cost.

Furthermore in middle part, it is depicted that the maximum percentage of the deviation for full two-connected and full one-connected is around 8% at network size with 11 nodes where full one-connected is as reference. While the deviation for basic connected is considered high at around 40% at network size with 7 nodes where basic one-connected is as reference.

Another metric used for measuring the performance of the model is the computational time as depicted in Figure 4.4 at lower part. Computational time tends to increase exponentially along with the increment network size. Two-connected models are using significantly less computational time compared to one-connected models. In extreme condition for example, at network size with 14 nodes, basic one-connected needs nearly 2000 seconds to solve the problem while for basic two-connected is only around 9 seconds.

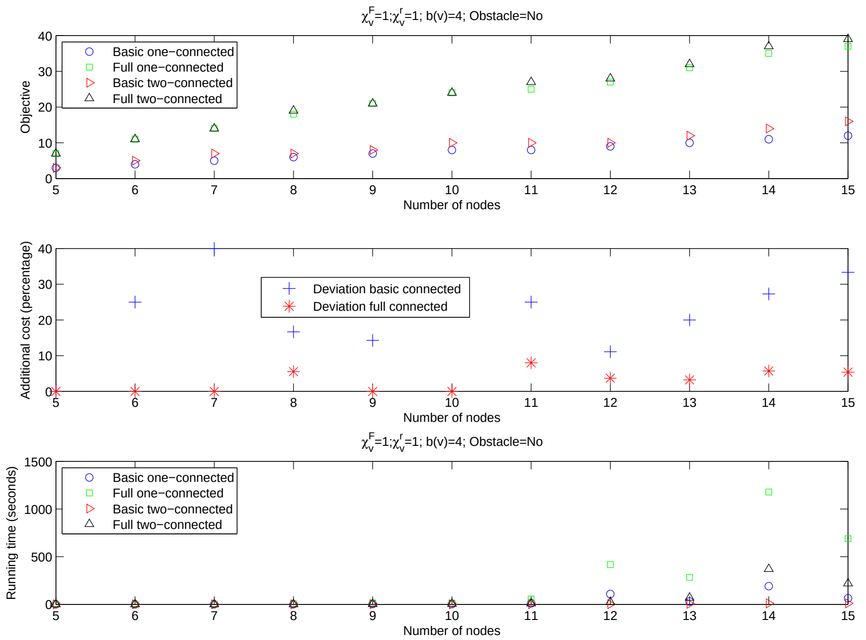

Figure 4.4: Computation time and objective cost of the models, case-1.

Figure 4.5 shows the optimized network topology. The transit nodes are not used in optimized topology since no customer premises in these nodes and been used as minimum as possible. Basic one-connected and basic two-connected model prefers to use more FSO links while full connected models prefers OF links if the cost of OF links same with FSO links. In this network examples, the cost of OF links are same with FSO links for the distance less than 1 km.

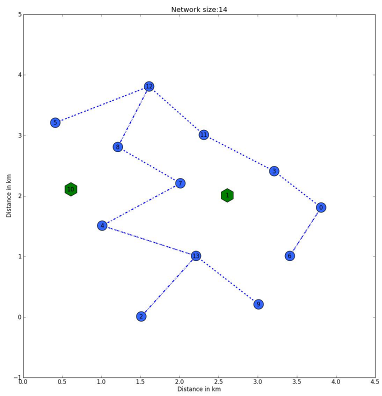

(a) Basic one-connected, case-1.

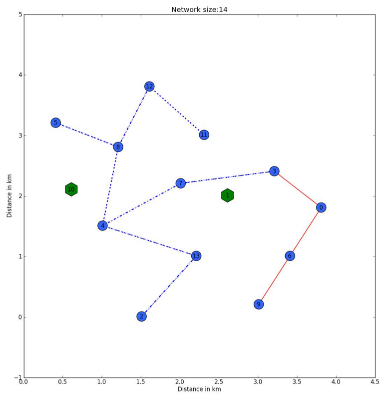

(b) Full one-connected , case-1.

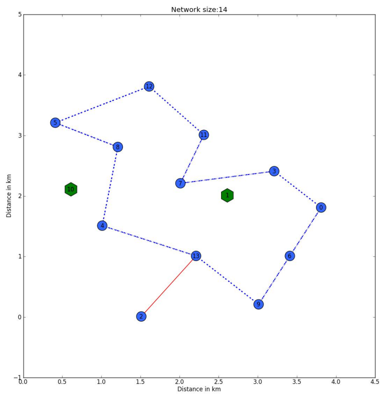

(c) Basic two-connected, case-1.

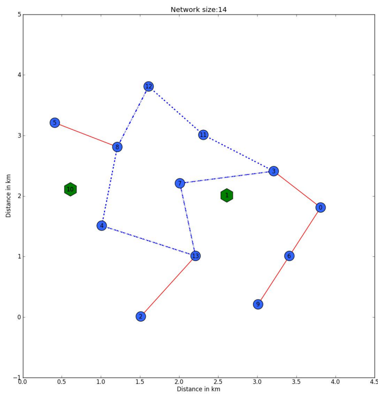

(d) Full two-connected, case-1.

Figure 4.5: Optimized topology for case-1, circle is node, diamond is transit node, dotted line is FSO link and solid line is OF link.

Since only few obstacles are present in the network topology hence they do not affect the performance of the models significantly.

4.2.2 Case-2: Cost χ_v^F= 3 , Cost χ_v^r=1, and $b(v)$=4

Adjust the cost of leased building to triple from previous case, one can see that the objective cost now is getting higher than the previous scenario as shown in Figure 4.6.

However, the computation time is increased nearly about 4 times for one-connected full model compared to previous case at network size equal to 14 nodes and going down after that. Comparing to case-1 the computation time for two-connected full is not significantly different.

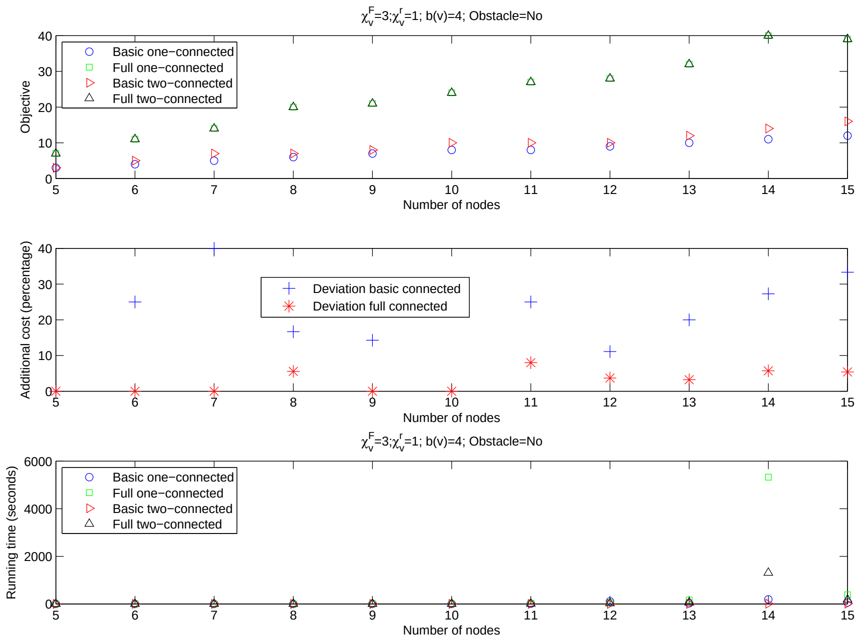

Figure 4.6: Computation time and objective cost of the models, case-2.

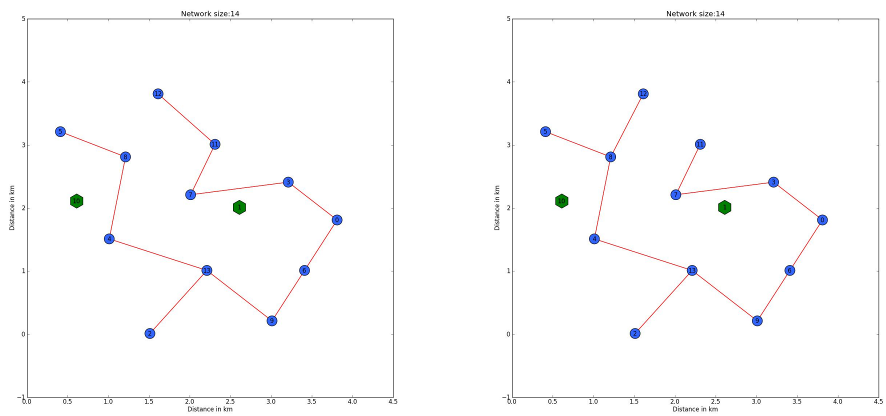

(a) Full one-connected, case-2. **(b)** Full two-connected, case-2.

Figure 4.7: Optimized topology for case2, circle is node, diamond is transit node, dotted line is FSO link and solid line is OF link.

Figure 4.5 indicates that adjustment of the leased building on the roof-top for FSO transceivers which causes the models to select most OF link as optimized topology. So it is reasonable that total objective cost for full connected models are more expensive than case1 scenario. This is also indicated by no deviation between full one-connected and two-connected as pointing out that OF links are most likely to be used. It is also reasonable that this adjustment is not affecting basic connected models.

4.2.3 Case-3: Cost χ_v^F= 1 , Cost χ_v^r=3, and $b(v)$=4

Furthermore, we investigated the case of increasing router costs. Figure 4.8 depicts that total cost of full-connected models are significantly more expensive, is approximately 50%, compared to previous two cases.

Running hours is dominated by full one-connected model, while computation time needed by full two-connected model is almost similar to case1.

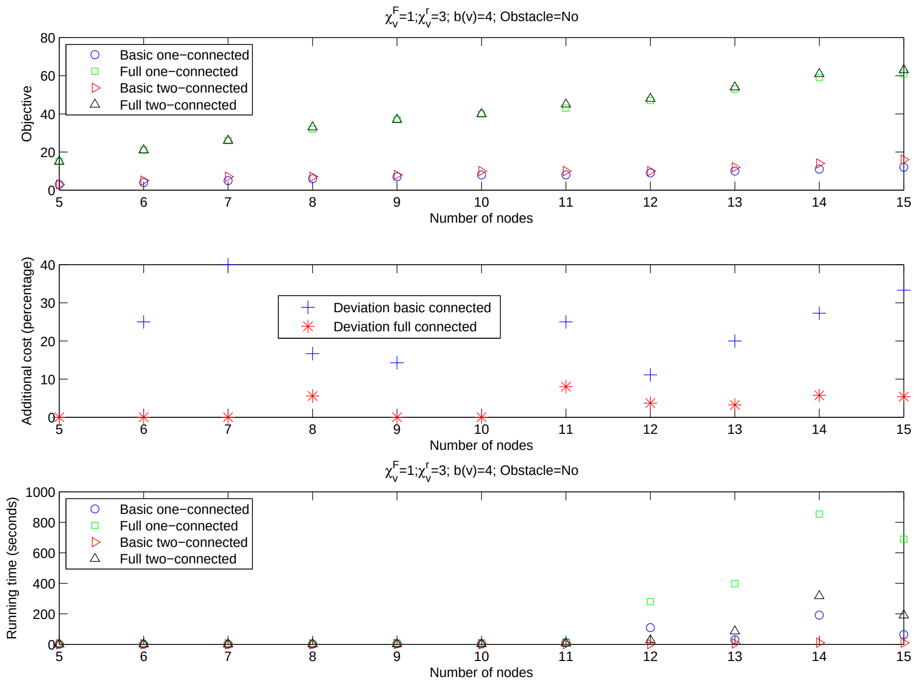

Figure 4.8: Computation time and objective cost of the models,case-3.

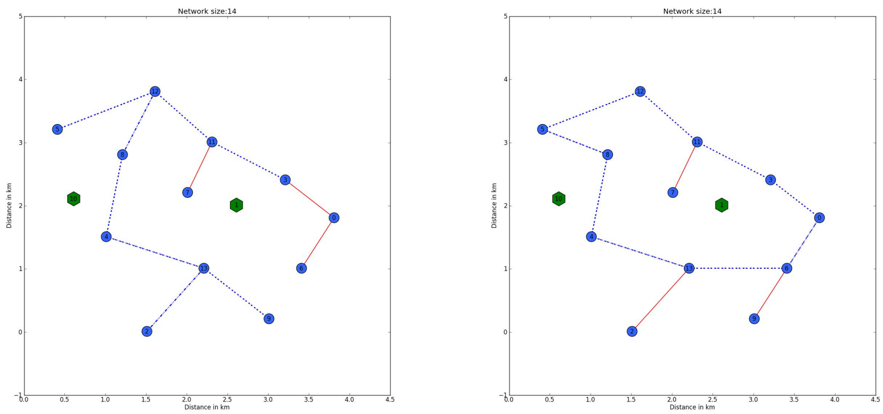

(a) Full one-connected, case-3. **(b)** Full two-connected, case-3.

Figure 4.9: Optimized topology for case3, circle is node, diamond is transit node, dotted line is FSO link and solid line is OF link.

Figure 4.9 shows that the topology is different from previous cases. Models are using more FSO links in optimized topology.

4.2.4 Case-4: Cost χ_v^F= 1 , Cost χ_v^r=3, and $b(v)$=2

As degree of FSO link is also one of the available parameters, in this case the degree is reduced to 2 FSO transceivers installed on the roof top. Although the overall performance is same with higher degree but the topology is changed as depicted in Figure 4.11 and it is observed that more OF links are used compared to case-3 with higher degree is.

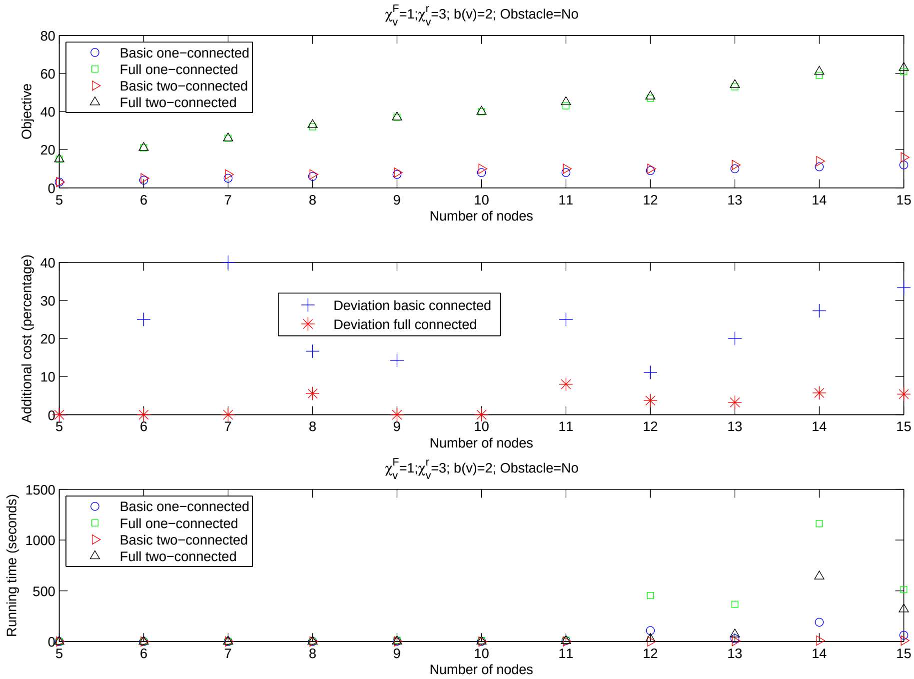

Figure 4.10: Computation time and objective cost of the models, case-4.

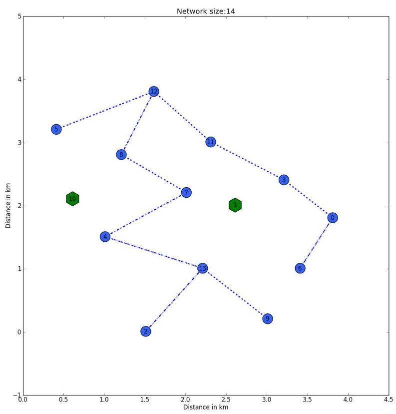

(a) Basic one-connected, case-4.

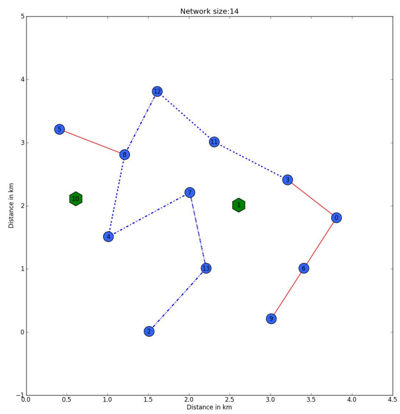

(b) Full one-connected , case-4.

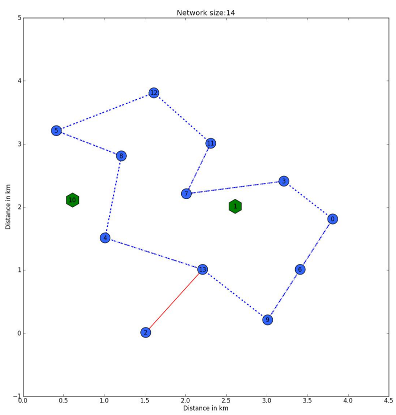

(c) Basic two-connected , case-4.

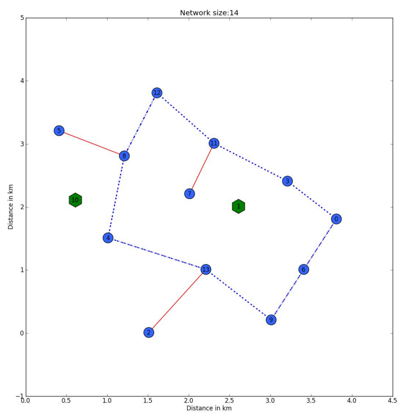

(d) Full two-connected , case-4.

Figure 4.11: Optimized topology for case1, circle is node, diamond is transit node, dotted line is FSO link and solid line is OF link.

4.2.5 Discussion of Results

As an observed in Figure 4.4, 4.6, 4.8, and 4.10 the computational time is increased in exponential fashion along with the increment of network complexity. This finding is in agreement with the proof shown in [1]. The nature of exponential computation time is due to the solver using Linear Programming based on Branch and Bound algorithm. During the experiments we also noticed that in some cases there are possible to have some feasible optimum solutions.

One can see that full two-connected is not significant costly compared to full one-connected model. The maximum additional cost needed for implementing full two-connected is around 10% of implementing full one-connected when the cost of leased building along with cost of routers are same with the cost of FSO link. For basic connected models seem that the maximum additional cost for implementing basic two-connected at certain network size is around 40%.

Models tend to use more OF links when the cost of leased building, χ_v^F, is higher compared to cost of routers, χ_v^r, as shown in Figure 4.7, but is not vice-verse. It is obvious that degree of FSO transceiver limit will change the optimized topology but will not merely increase the overall cost.

Construction of networks topology under investigation are very challenging. The generation is done by using random function of Python in two dimensional (x-y plane), furthermore there is a routine to verify none of node coordinate is overlapping each other. Also transit nodes are generated separately in the center of network topology. For simplicity, the cost of OF link is defined 1 unit (1 USD) for the distance less than 1 km, this definition affects the selection of optimization process.

Chapter 5

Conclusions, Contribution and Future Work

5.1 Conclusions

In conclusion, the numerical results show that the additional cost for implementing a more reliable solution, two-connected model, is less than double as compared to implementing one-connected model. As also noticed that the maximum cost of implementation for all models is the network configuration with all OF links usage.

The computational time for implementing two-connected models is not always longer than for one-connected models.

The most dominating parameter with respect to the overall objective cost in the models is the cost of a router, χ_v^r. This is reasonable because either OF or FSO transceiver must use the router to build a network. The fully connected models, either one-connected or two-connected, prefer OF links to FSO link in the case the cost of OF link and FSO link are same.

Increasing the price of the leased building, χ_v^F, will increase the cost of implementing FSO links since it will force the model to use more OF links whenever minimizing the overall objective cost. In general, the degree limit of FSO nodes does not affect the overall objective but it changes the network topology.

It is observed that there are more than one feasible solutions for the models in many cases.

According with the proof shown in [1], the solution of the optimization problem of this thesis is characterized by exponential running time.

5.2 Contribution

The main contribution of this thesis is in developing the Python scripts to be loaded to Gurobi optimizer for implementing the models and print out the results in files for a future use. This process is done automatically in Python environment.

To summarize the contribution is as follows.

- Developing the network models
- Designing the set of network generation
- Numerical experiments

- Investigate the effects of cost parameters for the models
- Finally draw the conclusions

5.3 Future work

It is observed that JTROP models are robust and reliable against single path failures. In order to increase the reliability even higher, some kind of model taking into account robustness to multiple failures of networks formulation could be considered.

The sets of data used are limited to 15 nodes. Since actual MAN implementation requires more nodes, there will be challenges to have more nodes investigated (e.g, 100 - 200 nodes) and some transit nodes in usage in order to have more general results. And finally, specification of the cost components should be made more detailed.

References

[1] M. Żotkiewicz, W. Ben-Ameur, and M. Pióro, "Finding Failure- disjoint paths for path diversity protection in communication networks," *IEEE Commun. Letters*, vol.?, No.?, February 2010.

[2] M. Pióro and D. Medhi. *Routing, Flow, and Capacity Design in Communication and Computer Networks.* Morgan Kaufman, San Fransisco, CA, USA, 2004.

[3] I. K. Son and S. Mao, "Design and Optimization of a Tiered Wireless Access Network," *IEEE INFOCOM*, 2010.

[4] Z. Ghassemlooy, W.O. Popoola, "Terrestrial Free-Space Optical Communications," pp. 355 - 392.

[5] I. I. Kim and E. Korevaar. *Availability of Free Space Optics (FSO) and hybrid FSO/RF systems.*

[6] I. I. Kim, B. McArthur, and E. Korevaar. *Comparison of laser beam propagation at 785 nm and 1550 nm in fog and haze for optical wireless communications.*

[7] H. Willebrand and B. S. Ghuman. *Free Space Optics: Enabling Optical Connectivity in Todays Networks.* Sams Publishing, USA, 2002.

[8] G. Keiser. *FTTX Concepts and Applications.* John Wiley & Sons, New Jersey, USA, 2006.

[9] Gurobi Optimization, Inc., "Gurobi Optimizer Reference Manual", 2012, http://www.gurobi.com.